

# High-statistics amplitude analyses of charmonium decays

Kirill Chilikin

Budker Institute of Nuclear Physics SB RAS, Novosibirsk, Russia

The 7th International Workshop  
on Future Tau-Charm Facilities  
(FTCF2025)  
25 November 2025

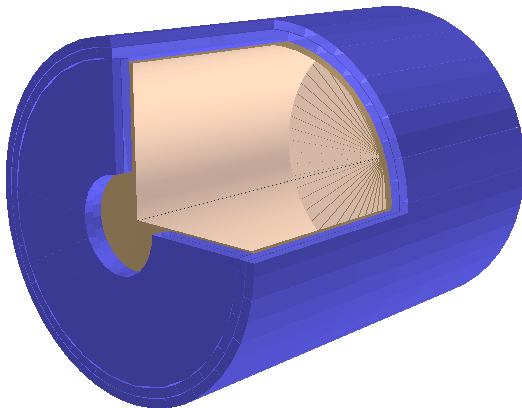


- VEPP-6 is a new collider and detector project at BINP focused on lower energies than the STCF,  $\sqrt{s} \sim 1.0 - 4.2 \text{ GeV}/c^2$ . Its general overview has been presented by Ivan Logashenko in the talk “Overview of collider projects at BINP” on 24 November.
- Preliminary accelerator parameters at the  $J/\psi$  energy are  $L = 1.4 \times 10^{34} \text{ cm}^{-2} \text{ s}^{-1}$  and  $\sigma_E/E = 0.8 \times 10^{-3}$ .
- The  $J/\psi$  cross section estimated from the BESIII cross section and parameters [NIM A **614**, 345 (2010)] is then  $\sim 2100 \text{ nb}$ , and the expected sample per effective year ( $1.0 \times 10^7 \text{ s}$ ) is  $\sim 3.0 \times 10^{11} J/\psi$  events if taking data at the  $J/\psi$  energy only.
- For further estimates in this talk, the total number of  $5.0 \times 10^{11} J/\psi$  events is used.



## VEPP-6 detector simulation

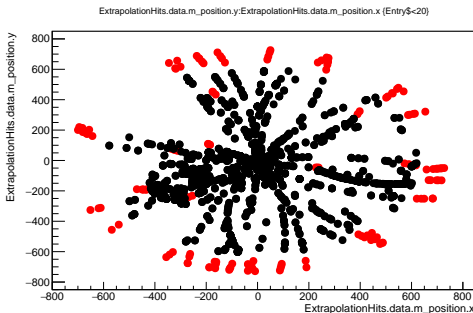
- The development of the VEPP-6 detector simulation has started from the Super  $c\text{-}\tau$  factory fast simulation [Comput. Softw. Big Sci. **8**, 1(2024)]. Overview of the software status has been presented by Daniil Zhadan today in the talk “Status of BINP SCT software” today.
- Fast simulation does not have  $\pi$ ,  $K$  decays or material interactions, which affect the signal in the PID system. Thus, the PID likelihoods there are not very realistic, and the first step for improvement is to add Geant4 simulation of the PID system.
- The primary option for the PID system is ASHIPH: aerogel with shifter with silicon photomultiplier. A talk about aerogel-based PID systems “Prospects of aerogel R&Ds at the BINP” will be given by Alexander Barnyakov on 26 November.



Only ASHIPH system has realistic geometry. The drift chamber is represented by a cylinder filled with air, outer detectors (calorimeter, muon system) are not implemented yet.



# Track extrapolation and reconstruction



- Tracking is performed by GenFit using Geant4 MC hits in the “drift-chamber” cylinder (black circles) and creates extrapolation hits when passing ASHIPH sensitive detectors (red circles). Track parameters are assigned from SCT fast simulation, while GenFit tracks are used for extrapolation to ASHIPH and reconstruction of ASHIPH PID likelihoods.
- Photons and drift-chamber PID likelihoods are from SCT fast simulation.

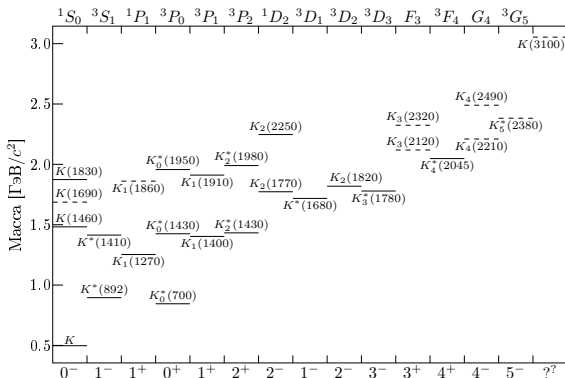


## $J/\psi$ as light-hadron factory

- When taking data at the  $J/\psi$  energy,  $J/\psi$  and  $\eta_c$  states are available, which are produced directly and in the  $J/\psi \rightarrow \eta_c \gamma$  decay, respectively. To study light hadrons, one can use:
  1. Hadronic decays of the  $J/\psi$  (discussed in this talk).
  2. Radiative decays of the  $J/\psi$ , e.g.  $J/\psi \rightarrow \gamma K \bar{K}$ .
  3. Hadronic decays of the  $\eta_c$ , e.g.  $\eta_c \rightarrow K^+ K^- \pi^0$ .
- The  $J/\psi$  hadronic decays can be used to study spectroscopy and decays of excited light-quark and strange mesons, the latter being considered as an example in the following. The primary tool of such studies is amplitude analysis.
- It is most simple to analyze three-body  $J/\psi$  decays (e.g.  $J/\psi \rightarrow K^+ K^- \pi^0$ ,  $J/\psi \rightarrow K^\pm K_S^0 \pi^\mp$ ), but the set of possible resonances there is limited by parity conservation.
- Thus, four-body  $J/\psi$  decays (e.g.  $J/\psi \rightarrow K^+ K^- \pi^+ \pi^-$ ,  $J/\psi \rightarrow K^\pm K_S^0 \pi^0 \pi^\mp$ ) need to be analyzed, too.
- Both three and four-body  $J/\psi$  decays have large branching fractions  $\gtrsim 10^{-3}$  and would provide extremely large signal statistics.



# Strange-meson spectrum



- Although strange-meson spectrum is known relatively well, some states shown by dashed lines need confirmation.
- The state  $K(1690)$  observed in a partial-wave analysis of the reaction  $K^- p \rightarrow K^- \pi^+ \pi^- p$  by COMPASS [arXiv:2504.09470] is of a special interest as it is not possible to find a corresponding state in potential models.



# Strange-meson decays

One can use decays  $X_{c\bar{c}} \rightarrow KK_J(\rightarrow f)$ , where  $X_{c\bar{c}}$  is a charmonium state,  $K_J$  is an excited  $K$  meson and  $f$  is the final state of its decay to study strange-meson spectroscopy.

State	$K\pi$	$K\eta$	$K\eta'$	$Kf_0(1370)$	$K\rho$	$K\omega$	$K\phi$	$Kf_2(1270)$	$K\gamma$	$K_0^*(1430)\pi$	$K^*(892)\pi$	$K^*(892)\pi\pi$	$K_2^*(1430)\pi$
$K_0^*(700)$	+	$M$	$M$	$P$	$P$	$P$	$P$	$P$	$P$	$P$	$P$	$M$	$P$
$K^*(892)$	+	$M$	$M$	$P$	$M$	$M$	$M$	$M$	+	$P$	$M$	$M$	$M$
$K_1(1270)$	$P$	$P$	$P$	+	+	+	$M$	$M$	+	+	+	-	$M$
$K_1(1400)$	$P$	$P$	$P$	+	+	+	+	$M$	+	-	+	-	$M$
$K^*(1410)$	+	-	$M$	$P$	-	-	+	$M$	-	$P$	+	-	$M$
$K_0^*(1430)$	+	+	+	$P$	$P$	$P$	$P$	$P$	$P$	$P$	$P$	$P$	$P$
$K_2^*(1430)$	+	+	-	$P$	+	+	-	$M$	+	$P$	+	+	$M$
$K(1460)$	$P$	$P$	$P$	-	+	-	+	$M$	-	+	-	-	$M$
$K^*(1680)$	+	+	-	$P$	+	-	+	$M$	-	$P$	+	-	-
$K_2(1770)$	$P$	$P$	$P$	-	-	+	+	+	-	-	+	-	+
$K_3^*(1780)$	+	+	-	$P$	+	-	-	-	-	$P$	+	-	-
$K_2(1820)$	$P$	$P$	$P$	-	-	+	+	+	-	-	+	-	+
$K(1830)$	$P$	$P$	$P$	-	+	-	+	-	-	-	-	-	-
$K_1(1910)$	$P$	$P$	$P$	-	+	-	+	-	-	-	-	-	-
$K_0^*(1950)$	+	-	-	$P$	$P$	$P$	$P$	$P$	$P$	$P$	$P$	$P$	$P$
$K_2^*(1980)$	-	+	-	$P$	-	-	-	-	-	$P$	-	-	-
$K_4^*(2045)$	+	-	-	$P$	-	-	-	-	-	$P$	-	+	-

Here “+” and “-” mean that the decay is observed or not observed, respectively,  $P$  denotes decays forbidden by parity and  $M$  stands for decays below the mass threshold.





## Main channels

One can derive the following conclusions from the decay table:

- The main channels for studies of the  $K_J^*$  with natural quantum numbers  $J^{(-1)^J}$  are two-body decays  $K\pi$ ,  $K\eta$ , and  $K\eta'$ . Decay of unnatural-parity ( $J^{(-1)^{J+1}}$ ) states to the same channels is forbidden by parity. This limits the number of possible contributions and simplifies the analysis. Thus, the main channels for studies of natural-parity states are  $J/\psi \rightarrow K\bar{K}\pi$ ,  $J/\psi \rightarrow K^+K^-\eta$ , and  $J/\psi \rightarrow K^+K^-\eta'$ .
- However, scalar states such as  $K_0^*(700)$  or  $K_0^*(1430)$  cannot be produced in the  $J/\psi$  decays because the decay  $J/\psi \rightarrow K_0^*\bar{K}$  is forbidden by parity. It is necessary to use  $\eta_c$  decays to the same final states to study them.
- To study unnatural-parity states, it is necessary to use three-body final states such as  $K\pi\pi$  taking all possible intermediate resonances into account. Thus, main channels for their studies are  $J/\psi \rightarrow K\bar{K}\pi\pi$  and  $J/\psi \rightarrow K\bar{K}K\bar{K}$  for  $K_J \rightarrow K\phi$ .



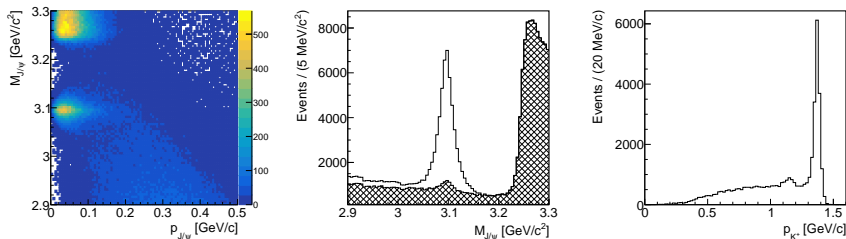
## MC sample and reconstruction

- A sample consisting of  $500 \times 10^6$   $J/\psi$  events has been simulated. It does not include annihilation into light quarks or backgrounds.
- The simulated sample is used to test PID performance and estimate the expected sizes of the signal samples for main channels. Particularly, three-body  $J/\psi$  decays are reconstructed:  
 $J/\psi \rightarrow \pi^+ \pi^- \pi^0$ ,  $J/\psi \rightarrow K^+ K^- \pi^0$ ,  $J/\psi \rightarrow K^\pm K_S^0 \pi^\mp$ .
- Signal events are identified by  $M_{J/\psi}$  and  $p_{J/\psi}$  before the  $J/\psi$  mass fit. The initial requirements are  $2.9 < M_{J/\psi} < 3.3 \text{ GeV}/c^2$  and  $p_{J/\psi} < 0.5 \text{ GeV}/c$ .
- The angular acceptance in Super  $c\text{-}\tau$  factory fast simulation is too optimistic for the new detector. An additional requirement on polar angle is imposed:  $|\cos \theta| < \cos 18^\circ$ .



## PID requirements

Results for  $J/\psi \rightarrow K^+ K^- \pi^0$  for a limited sample of  $20 \times 10^6$   $J/\psi$  events are presented below; PID requirements are not applied except for the  $K$  momentum plot. The resonance fractions are from BESIII analysis [Phys. Rev. D **100**, 032004 (2019)]. The mass plot is for  $p_{J/\psi} < 0.25$  GeV/c, the hatched histogram is events that are removed by PID selection.

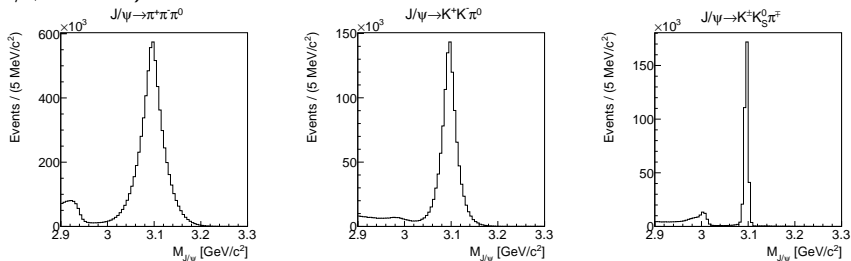


- A PID system with  $\pi/K$  separation up to about 1.45 GeV/c is necessary for amplitude analyses of the  $J/\psi$  decays.



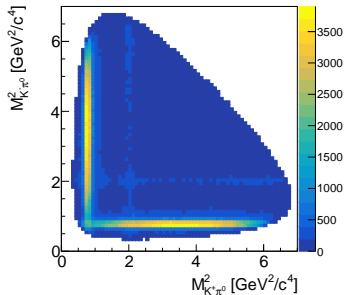
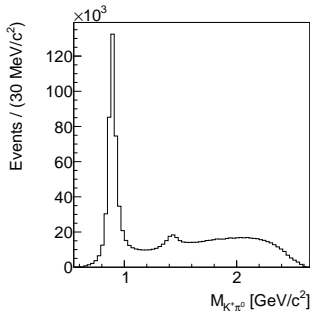
# PID requirements

PID requirements are now applied for channels with  $K^\pm$ . The resulting mass plots for  $p_{J/\psi} < 0.25 \text{ GeV}/c^2$  for full simulated sample ( $500 \times 10^6$   $J/\psi$  events) are:



- After application of PID requirements, the background level becomes small. Thus, ASHIPH would provide a good performance for  $J/\psi$  decays.

The decay  $J/\psi \rightarrow K^+ K^- \pi^0$  is considered as an example hereinafter. The data sample for amplitude analysis is selected by applying  $M_{J/\psi} > 3.02 \text{ GeV}/c^2$ ,  $p_{J/\psi} < 0.25 \text{ GeV}/c$ , and PID for kaons.



The number of selected events is  $\sim 1100000$ . For a sample of  $5.0 \times 10^{11}$   $J/\psi$  events,  $\sim 1.0 \times 10^9$  events in the signal region are expected.



## Technical requirements on fit

- The signal density is normalized using MC integration and needs to be calculated for MC events, too. One should increase the estimate for number of events at least an order of magnitude to take MC into account.
- Thus, for a sample of  $5.0 \times 10^{11}$   $J/\psi$  events,  $\sim 1.0 \times 10^{10}$  data and MC events need to be processed by the fitting program.
- Large number of events results in large necessary CPU time. Optimization is always necessary: low-level SIMD parallel calculations and calculation of likelihood gradient to reduce the necessary number of function calls.
- The size of buffers for precalculated values (e.g. angular distribution) is 75 Gb per single 64-bit number for  $1.0 \times 10^{10}$  events, multiple values need to be stored. The memory size is much larger than typical memory per core at clusters, parallel calculations are necessary.



## Technical requirements on fit

- The signal density is normalized using MC integration and needs to be calculated for MC events, too. One should increase the estimate for number of events at least an order of magnitude to take MC into account.
- Thus, for a sample of  $5.0 \times 10^{11}$   $J/\psi$  events,  $\sim 1.0 \times 10^{10}$  data and MC events need to be processed by the fitting program.
- Large number of events results in large necessary CPU time. Optimization is always necessary: low-level SIMD parallel calculations and calculation of likelihood gradient to reduce the necessary number of function calls.
- The size of buffers for precalculated values (e.g. angular distribution) is 75 Gb per single 64-bit number for  $1.0 \times 10^{10}$  events, multiple values need to be stored. The memory size is much larger than typical memory per core at clusters, parallel calculations are necessary.

It is necessary to develop a software library for amplitude analyses that is able to satisfy the technical requirements.



## Signal amplitude for $J/\psi \rightarrow K^+ K^- \pi^0$

The amplitude of the decay  $J/\psi \rightarrow K_J^* \bar{K}$  is

$$\begin{aligned} A &= \phi_{\alpha_1}^{(J/\psi)} \epsilon_{\alpha_1 \alpha_2 \alpha_3 \alpha_4} p_{J/\psi}^{\alpha_4} (L_{(J)}^{(J/\psi)})_{\beta_1 \dots \beta_{J-1}}^{\alpha_2} (L_{(J)}^{(K_J^*)})^{\alpha_3 \beta_1 \dots \beta_{J-1}} \\ &= \phi_{\alpha_1}^{(J/\psi)} \epsilon_{\alpha_1 \alpha_2 \alpha_3 \alpha_4} p_{J/\psi}^{\alpha_4} q_{J/\psi}^{\alpha_2} q_{K_J^*}^{\alpha_3} T_J, \end{aligned} \quad (1)$$

where  $T_J$  is the angular part. Calculations are carried out using the program FORM [J. A. M. Vermaseren, (2000), arXiv:math-ph/0010025] and result in

$$T_1 = 1,$$

$$T_2 = (\tilde{q}_{J/\psi}, \tilde{q}_{K_J^*}),$$

$$T_3 = (\tilde{q}_{J/\psi}, \tilde{q}_{K_J^*})^2,$$

$$T_4 = (\tilde{q}_{J/\psi}, \tilde{q}_{K_J^*})^3 + \frac{3}{7} (\tilde{q}_{J/\psi}, \tilde{q}_{K_J^*}) \left[ \frac{(p_{J/\psi}, \tilde{q}_{K_J^*})^2 \tilde{q}_{J/\psi}^2}{p_{J/\psi}^2} + \frac{(\tilde{q}_{J/\psi}, p_{K_J^*})^2 \tilde{q}_{K_J^*}^2}{p_{K_J^*}^2} \right]. \quad (2)$$





## Event buffer size

For any amplitude, including model-independent partial-wave analysis, one has to include

1. The vector-product part of the amplitude is equal to  $\epsilon_{\alpha_1\alpha_2\alpha_3\alpha_4} p_{K^+}^{\alpha_2} p_{K^-}^{\alpha_3} p_{\pi^0}^{\alpha_4}$ , it is the same for all 3 decay chains: 3 values, but reduces to 2 for signal density due to the  $J/\psi$  polarization vector.
2. Angular part: generally, 3 values for contributions with each spin greater than 2: 12 values for spins up to 5. Reduces to 8 as  $T_3$  can easily be calculated from  $T_2$  and only odd spins are possible for a particle-antiparticle pair  $K^+$  and  $K^-$ .

If model-dependent resonance shapes are used, then one needs to include

1. Invariant mass of each 2-particle combination: 3 values.
2. Optionally, daughter momenta in intermediate decays used in formfactors (can also be computed from invariant masses): 6 values.

In total, there are at least 10 variables per event to be stored if spins up to 5 are included. For  $10^{10}$  events, the required memory size is 745 GB.



## Event buffer size

For any amplitude, including model-independent partial-wave analysis, one has to include

1. The vector-product part of the amplitude is equal to  $\epsilon_{\alpha_1\alpha_2\alpha_3\alpha_4} p_{K^+}^{\alpha_2} p_{K^-}^{\alpha_3} p_{\pi^0}^{\alpha_4}$ , it is the same for all 3 decay chains: 3 values, but reduces to 2 for signal density due to the  $J/\psi$  polarization vector.
2. Angular part: generally, 3 values for contributions with each spin greater than 2: 12 values for spins up to 5. Reduces to 8 as  $T_3$  can easily be calculated from  $T_2$  and only odd spins are possible for a particle-antiparticle pair  $K^+$  and  $K^-$ .

If model-dependent resonance shapes are used, then one needs to include

1. Invariant mass of each 2-particle combination: 3 values.
2. Optionally, daughter momenta in intermediate decays used in formfactors (can also be computed from invariant masses): 6 values.

In total, there are at least 10 variables per event to be stored if spins up to 5 are included. For  $10^{10}$  events, the required memory size is 745 GB.

The library should be able to perform parallel calculations using hundreds of GB of data.



Development of dedicated amplitude-analysis library is ongoing. It performs minimization of likelihood of the general form

$$\mathcal{F} = \sum_a \sum_i -2 \ln \left[ (f_S)_a \frac{S_a(\Phi_i, p_S)}{\sum_j w_j S_a(\Phi_j, p_S)} + \sum_k (f_B^{(k)})_a \frac{B_a^{(k)}(\Phi_i, p_B^{(k)})}{\sum_j w_j B_a^{(k)}(\Phi_j, p_B^{(k)})} \right] + \sum_l C_l(p_S^{(n_l)}) + C(p_S), \quad (3)$$

where  $a$  is simultaneous-fit point number, indices  $i$  and  $j$  run over data and normalization MC events, respectively,  $f_S$  is the signal fraction,  $f_B^{(k)}$  is the fraction of background source  $k$ ,  $S$  and  $B^{(k)}$  are signal and background density functions, respectively,  $\Phi$  is the phase space,  $p_S$  and  $p_B^{(k)}$  are signal and background parameters, respectively,  $w_j$  are MC event weights, and  $C_l$  and  $C$  are constraint functions.



- In case of extended unbinned maximum likelihood fit the likelihood has an additional term

$$\Delta\mathcal{F} = 2(N - N_{\text{data}} \ln(N)), \quad (4)$$

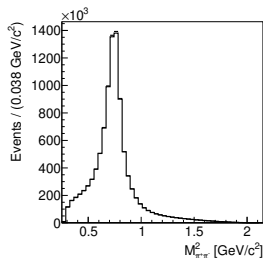
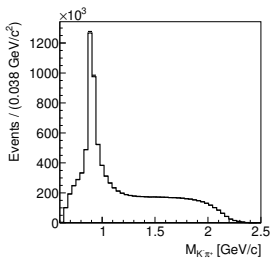
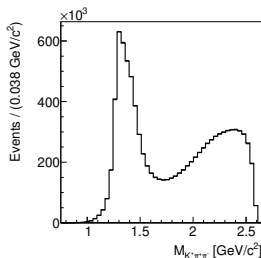
where  $N$  is the number of events (fit parameter) and  $N_{\text{data}}$  is the number of observed events.

- Similar minimization with gradient of likelihood is possible. The user needs to calculate the gradient of signal density  $S$  manually.
- The signal and background density functions are calculated for short fixed-length arrays rather than single numbers. This allows to compile their code into SIMD instruction, performing low-level parallel calculations. The library provides basic physical and mathematical functions in vectorized form to assist density-function programming.



## Example fit

- The original plan was to perform an example analysis using actual VEPP-6 simulation. Unfortunately, it was not ready in time.
- An existing example from VECAMPFIT,  $e^+e^- \rightarrow K^+K^-\pi^+\pi^-$ , is adapted instead using the  $J/\psi$  energy and higher statistics.
- The model includes only two resonances,  $K_1(1270)^+$  and  $K_1(1400)^+$ . The signal density is calculated using the helicity formalism. The background is described by a second-order polynomial.
- $1.0 \times 10^7$  signal events and  $1.0 \times 10^8$  normalization MC events are used. Fit needs 50 GB RAM, tested using from 16 to 32 cores.





# Conclusions

1. Test simulation and reconstruction of several  $J/\psi$  decays at VEPP-6 has been performed. For that:
  - Hybrid simulation of the VEPP-6 detector has been implemented. It includes Geant4 simulation of very simple geometry, MC-based tracking, track extrapolation, and ASHIPH PID likelihood reconstruction.
  - Analysis package has been updated to handle the required reconstruction procedure.

It shows that ASHIPH system would provide a good PID performance for amplitude analyses of  $J/\psi$  decays.

2. Due to very large number of signal events, amplitude analysis of  $J/\psi$  decays requires a special library that would be able to handle fits with parallel calculations. Development of such library `VECAMPFIT` is ongoing (originally for an ongoing amplitude analysis at Belle II, but will be also useful for VEPP-6 or STCF). First public version and publication are expected soon.

BACKUP



## Covariant formalism with specific partial waves

Main reference is S. U. Chung, “Helicity coupling amplitudes in tensor formalism”, Phys. Rev. D **48**, 1225 (1993), [Erratum: Phys. Rev. D **56**, 4419 (1997)] and a good application example is LHCb Collaboration, “Amplitude analysis of  $B^+ \rightarrow \psi(2S)K^+\pi^+\pi^-$  decays”, JHEP **01**, 054 (2025). The amplitude of the decay  $R \rightarrow A + B$  is given by

$$A = \phi_{\mu_R}^{(R)} E(J_R, L_{AB}, S_{AB}) L_{\mu_L}^{AB} P_{AB}^{\mu_A \mu_B} E(S_{AB}, J_A, J_B) \phi_{\mu_A}^{(A)*} \phi_{\mu_B}^{(B)*}, \quad (5)$$

where  $\phi$  is the wave function of the resonance specified by the superscript,  $L_{\mu_L}^{AB}$  is angular-momentum tensor,  $P_{AB}^{\mu_A \mu_B}$  is projection operator, and

$$E(J_1, J_2, J_3) = \begin{cases} 1 & \text{if } J_1 + J_2 + J_3 \text{ is even,} \\ \epsilon_{\alpha_1 \alpha_2 \alpha_3 \alpha_4} P_R^{\alpha_4} & \text{if } J_1 + J_2 + J_3 \text{ is odd.} \end{cases} \quad (6)$$





# Projection operators

The general expression for projection operators has been calculated in [Phys. Rev. **106**, 345 (1957)]:

$$P_{\alpha_1 \dots \alpha_J \beta_1 \dots \beta_J}^{(J)} = \frac{(-1)^J}{J!^2} \sum_{P(\alpha), P(\beta)} \left[ \prod_{i=1}^J \tilde{g}_{\alpha_i \beta_i} + a_1 \tilde{g}_{\alpha_1 \alpha_2} \tilde{g}_{\beta_1 \beta_2} \prod_{i=3}^J \tilde{g}_{\alpha_i \beta_i} + \dots \right. \\ \left. + \begin{cases} a_{J/2} \tilde{g}_{\alpha_1 \alpha_2} \tilde{g}_{\beta_1 \beta_2} \dots \tilde{g}_{\alpha_{J-1} \alpha_J} \tilde{g}_{\beta_{J-1} \beta_J} & \text{for even } J \\ a_{(J-1)/2} \tilde{g}_{\alpha_1 \alpha_2} \tilde{g}_{\beta_1 \beta_2} \dots \tilde{g}_{\alpha_{J-2} \alpha_{J-1}} \tilde{g}_{\beta_{J-2} \beta_{J-1}} \tilde{g}_{\alpha_J \beta_J} & \text{for odd } J \end{cases} \right], \quad (7)$$

where  $P(\alpha)$  and  $P(\beta)$  are all  $\alpha$  and  $\beta$  index permutations, respectively,

$$\tilde{g}_{\alpha\beta} = g_{\alpha\beta} - \frac{p_\alpha p_\beta}{p^2}, \quad (8)$$

and the coefficients  $a_i$  are given by

$$a_i = \frac{J!}{(-2)^i i! (J-2i)!} \frac{1}{(2J-1)(2J-3) \dots (2J-2i+1)}. \quad (9)$$

The factor  $(-1)^J$  is added to follow the sign convention of [Phys. Rev. D **48**, 1225 (1993)].



# Angular-momentum tensors

The angular-momentum tensors are given by

$$L_{(J)}^{\alpha_1 \dots \alpha_J} = P_{(J)}^{\alpha_1 \dots \alpha_J \beta_1 \dots \beta_J} q_{\beta_1} \dots q_{\beta_J}. \quad (10)$$

The explicit expressions for the angular-momentum tensors are

$$\begin{aligned} L_{(0)} &= 1, \\ L_{(1)}^{\alpha_1} &= \tilde{g}^{\alpha_1 \beta_1} q_{\beta_1} = q^{\alpha_1} - \frac{(p, q)}{p^2} p^{\alpha_1} = \tilde{q}^{\alpha_1}. \end{aligned} \quad (11)$$

For spin 2

$$L_{(2)}^{\alpha_1 \alpha_2} = \tilde{q}^{\alpha_1} \tilde{q}^{\alpha_2} - \frac{1}{3} (\tilde{q}, \tilde{q}) \tilde{g}^{\alpha_1 \alpha_2}, \quad (12)$$

where the scalar product is

$$(\tilde{q}, \tilde{q}) = q^2 - 2 \frac{(p, q)}{p^2} (p, q) + \frac{(p, q)}{p^2} p^2 = q^2 - \frac{(p, q)^2}{p^2}. \quad (13)$$

For spin 3

$$L_{(3)}^{\alpha_1 \alpha_2 \alpha_3} = \tilde{q}^{\alpha_1} \tilde{q}^{\alpha_2} \tilde{q}^{\alpha_3} - \frac{1}{5} (\tilde{q}, \tilde{q}) (\tilde{g}^{\alpha_1 \alpha_2} \tilde{q}^{\alpha_3} + \tilde{g}^{\alpha_1 \alpha_3} \tilde{q}^{\alpha_2} + \tilde{g}^{\alpha_2 \alpha_3} \tilde{q}^{\alpha_1}). \quad (14)$$